Consistency Assessments of the Land Cover Products on the Tibetan Plateau

Liping Cai, Shanshan Wang, Lizhi Jia, Yijia Wang, Hui Wang, Donglin Fan, and Lin Zhao

***Abstract*—Land cover (LC) and LC change information are essential data in terrestrial surface research. However, the LC products are highly inconsistent, especially in the mountainous area. Most LC assessment studies focused on the consistency of spatial patterns, while ignoring the consistency of change and elevation heterogeneity. In this article, four LC products were assessed for spatiotemporal consistency on the Tibetan Plateau (TP), including the moderate resolution imaging spectroradiometer LC (MCD12Q1), the climate change initiative LC (CCI-LC), the 30-meter global land cover (Globeland30) and the multiperiod land use/ LC remote sensing monitoring database in China. The impact of elevation on the consistency of multiple LC products across spatiotemporal scales was further analyzed. The spatial consistency of the three and more products was about 70%, with higher consistency for grassland and bare land and lower consistency for wetland and shrubland on the TP. Globeland30 and CCI-LC were better than others for overall monitoring, with the inconsistency of less than 45% by Google Earth dataset validation. The temporal change consistency of the four LC products was less than 10%. With increasing elevation, the average spatial consistency decreased and the LC change area and temporal change consistency increased. There is a high inconsistency of LC changes on the TP in existing commonly used products, demonstrating the need to develop high-quality LC products in long time series.**

***Index Terms*—Land cover (LC) pattern, LC product, spatial consistency, temporal consistency, Tibetan Plateau.**

I. Introduction

RESEARCH about land cover (LC) and its change has become one of the key themes in global change and sustainable development research, providing an entry point for understanding the relationship between human beings and the natural environment [1], [2]. As important terrestrial monitoring data, the LC provides basic information about the biophysical properties of the earth's surface [3], [4]. LC change has perturbed biodiversity [5], [6], affected carbon emission [7], and altered the provision of ecosystem services [8], [9]. Accurate LC change information can help humanity successful tackle a vast of globalized challenges, such as urban expansion [10], [11], climate change [12], [13], and disaster prevention and mitigation [14], [15]. It is due to the widespread use of LC and its change information that the monitoring techniques of LC are also evolving rapidly. With the increase of LC products, the selection of valuable products for regional studies is a common concern.

Since the first satellite remote global LC map was produced, with the improvement of satellite-based earth observation technology and the development of extraction algorithms, LC products are emerging [16], [17]. There are several common sets of global and regional LC products. The moderate-resolution imaging spectroradiometer (MODIS) *LC* dataset produced by NASA with a spatial resolution of 500 m, is a continuous LC product with a one-year interval [18]. The climate change initiative LC (CCI-LC) dataset has a spatial resolution of 300 m with 22 types of LC [18]. The 30-m global land cover (Globeland30) has a high resolution of 30 m and was produced by the National Geomatics Center of China [19]. The multiperiod land use/LC remote sensing monitoring database in China (CNLUCC) is produced by the Institute of Geomatics Science and Natural Resources Research with a resolution of 30 m (http://www.resdc.cn) [20]. The availability of these LC products has provided a database for other LC-based studies [21]. However, there are large inconsistencies between different LC products due to different types of sensors, shooting angles, deformation levels, and interpretation methods [22]. Low precision landcover data will result in greater errors, leading to greater uncertainty in many researches [23]. Therefore, the selection of LC products is of great significance to regional studies.

Despite the relatively high accuracies provided by LC products through self-evaluation, some studies found a significant inconsistency of results when verifying current LC products using different reference datasets or samples in different places [24]. By analyzing the spatial consistency of the five LC products at the global and continental levels, it is found that the spatial consistency of the five LC sets was relatively low and characterized by spatial heterogeneity [25]. The analysis of the consistency of the five LC products in China revealed that the areas of spatial inconsistency were mainly distributed in the transition areas of topographic gradients, such as the southwest

Manuscript received 11 May 2022; revised 6 June 2022 and 20 June 2022; accepted 26 June 2022. Date of publication 5 July 2022; date of current version 21 July 2022. This work was supported in part by the Strategic Priority Research Program of the Second Tibetan Plateau Scientific Expedition and Research Program under Grant 2019QZKK0405, and in part by the Shandong Provincial Natural Science Foundation under Grant ZR2019BD045. *(Corresponding author: Lizhi Jia.)*

Liping Cai, Shanshan Wang, Hui Wang, Donglin Fan, and Lin Zhao are with the School of Geography and Tourism, Qufu Normal University, Rizhao 276800, China (e-mail: cumtcailp@126.com; qfsdwss@163.com; 1012959497@qq.com; calm_dl_fan@163.com; linzhao@qfn.edu.cn).

Lizhi Jia is with the Lasa Plateau Ecosystem Research Station, Key Laboratory of Ecosystem Network Observation and Modeling, Institute of Geographic Sciences and Natural Resources Research, Chinese Academy of Sciences, Beijing 100101, China (e-mail: jializhi@igsnrr.ac.cn).

Yijia Wang is with the State Key Laboratory of Earth Surface Processes and Resource Ecology, Faculty of Geographical Science, Beijing Normal University, Beijing 100875, China (e-mail: yijiawang27@mail.bnu.edu.cn).

Digital Object Identifier 10.1109/JSTARS.2022.3188650

TABLE I
BASIC INFORMATION ON FOUR LAND COVER PRODUCTS

	MCD12Q1	CCI-LC	Globeland30	CNLUCC
Spatial Resolution (m)	500	300	30	1000
Overall accuracy (%)	71.60	Validation in process	2000: 78.60 2010: 80.50	88.95
Sensor	MODIS	MERIS Full and Reduced Resolution/SPOT VGT	Landsat-TM, ETM7, HJ-1A/b/	Landsat-TM/ Landsat8
Classification Technique	Supervised classification	Unsupervised classification	Supervised classification	Supervised classification
Classification Scheme	IGBP (17 classes)	UN-LCC （22 classes）	（10 classes）	（25 classes）
Period of data acquisition	2001 – 2019	1992 – 2020	2000、2010、2020	2000、2005、2010、2015、2018、2020
Institution	National Aeronautics and Space Administration (NASA)	European Space Agency (ESA)	National Geomatics Center of China (NGCC)	Institute of Geographic Sciences and Natural Resources Research (IGSNRR)
Source	https://ladsweb.modaps.eosdis.nasa.gov/	https://www.esa-landcover-cci.org/	http://www.globeland30.com	http://www.resdc.cn/Datalist1.aspx?

region of China [26]. The consistency analysis of three LC products with a resolution of 30 m over the Indonesian region found that the area with high consistency occupied only 58% of the total Indonesian area [27]. The overall accuracy between the four LC products ranged from 56.30% to 68.8% in the African [28]. However, most of these studies focused on the consistency of spatial patterns while ignoring the consistency of LC change. As the highest plateau in the world, the Tibetan Plateau (TP) is more ecologically fragile and sensitive than other regions [29]. Under the background of global warming, the ecological problems caused by land use change will become more obvious [30]. Wang *et al.* [31] found significant LC changes on the TP from 2000 to 2015 by using MODIS, in which bare land and grassland areas decreased significantly, urban areas expanded at a rate of 41.2% and glaciers concentrated in the south and southeast retreated by about 3.4%. Using China cover LC data, Jiang *et al.* found that the area of glaciers decreased from 2.72% to 2.646% and the area of rivers and lakes expanded significantly. Wang *et al.* [32] found that nearly 38.8% of the grassland on the TP underwent degradation from 2001 to 2013 by coupling remote sensing and meteorological data. However, it is unclear whether the results of the abovementioned studies are comparable due to inconsistencies in LC products.

Aiming at the uncertain gaps in findings on the LC on the TP under different products, this article was to verify the spatiotemporal consistency of four mainstream LC products of MCD12Q1, CCI-LC, Globeland30, and CNLUCC in 2000, 2010, and 2020, respectively. Three scientific questions were attempted to be answered: 1) LC patterns of four LC products in the TP and their spatial consistency; 2) LC changes of four LC products in the TP and their change consistency; and 3) elevational difference of spatiotemporal consistency of four LC products on the TP.

II. STUDY AREA AND DATA

A. Study Area

As the highest plateau in the world, the average altitude of the TP exceeds 4000 m [33]. It has a huge system of mountain ranges, which contains mountain systems and plateau surfaces (see Fig. 1). The climate of TP is complex and diverse, characterized by low temperatures, small annual differences [34]. The TP is not only the initiator and regulator of climate change in the northern hemisphere but also has obvious sensitivity, advancement, and regulation to the global climate. The rate of warming in the TP region was more pronounced than in other regions [35]. Over the past 50 years, the rate of warming has been rapid, reaching 0.4 °C/10yr [36] and the rate of warming in winter has even reached twice the annual average [37], [38].

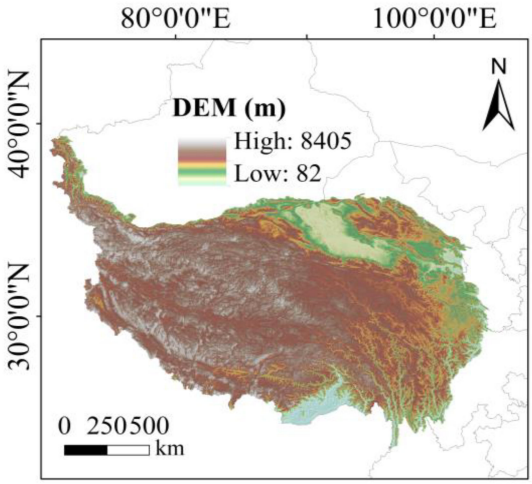

Fig. 1. Location and topographic map of the TP.

B. LC Products

Four LC products (MCD12Q1, CCI-LC, Globeland30, CNLUCC) were chosen for consistency assessment on the TP (see Table I). Since the MCD12Q1 has been produced since 2001, data for 2020 has not been released yet. Therefore, 2001 and 2019 data are used instead of 2000 and 2020 data, respectively.

TABLE II
CLASSIFICATION CONSOLIDATION SCHEME USED FOR LAND COVER PRODUCTS (THE NUMBER IS THE LAND COVER CLASSIFICATION IN EACH PRODUCT.)

	MCD12Q1	Globeland30	CCI-LC	CNLUCC
Forest	1/2/3/4/5	20	40/50/60/61/62/70/71/72/80/81/ 82/90/100/160/170	21/23/24
Shrubland	6/7	40	120/121/122	22
Grassland	8/9/10	30	110/130	31/32/33
Cultivated land	12/14	10	10/11/12/20/30	11/12
Wetland	11	50	180	46/64
Water bodies	17	60	210	41/42/43
Artificial surfaces	13	80	190	51/52/53
Permanent snow and ice	15	100	220	44
Bare land	16	90	140/150/151/152/153/200/201/202	61/62/63/65/66/67

III. METHODS

A. Data Preprocessing

Four LC products were distributed in different geographic systems and spatial resolutions [39]. To compare the consistency of the four datasets, we preprocessed the original products by transforming projections, unifying resolutions, and merging classification systems. The WGS84 datum and Albers projection (the central longitude of the projection was 105°E and the double standard latitude lines were 25°N and 47°N) were used as the spatial framework for all data. LC products were converted into 1 km resolution using the nearest neighbor method [40], [41]. Among the four LC products, the Globeland30 product with the least number of LC types in TP. The other three LC products were harmonized LC classification system according to the LC types of Globeland30. Table II showed the classification scheme of the multisource LC products.

B. Data Analysis

1) Classification Accuracy Analysis: The confusion matrix, based on LC types, is still a widely used metric to assess product accuracy [42], [43]. It includes the overall accuracy (OA), producer accuracy (PA), user's accuracy (UA) and kappa coefficient to assess the accuracy of remote images [44], [45].

The corresponding information and accuracy index of pixels between two of the four LC products could be obtained by using the confusion matrix. OA and PA were used as the main evaluation factors. OA refers to the ratio of the number of correctly classified samples to the total number of samples. This index measures the proportion of the overall correct classification of test data. PA is the ratio of the number of pixels correctly classified as class *i* in the data to be evaluated to the number of pixels of class *i* in the reference data. The formulas are as follows:

$$\mathrm{OA} = \frac{\sum_{i=1}^{r} x_{ii}}{N} \times 100\% \tag{1}$$

$$\mathrm{PA} = \frac{x_{ii}}{x_{+i}} \times 100\% \tag{2}$$

where N is the total number of pixels, r is the number of LC types, x_{ii} is the number of pixels correctly classified, and x_{+i} is the number of pixels of a particular type in the reference data.

2) Spatial Consistency Analysis: The LC consistency map of the TP was obtained by overlaying four LC product maps of the same year, which indicated the level of consistency among these LC products. First, the four LC products were set to the same number of rows and aligned by mask extraction in the ArcGIS (v.10.8). Then, the four LC products were superimposed in the raster calculator tool using (3) to obtain a consistent map. Finally, the consistency map was classified as 1) the LC types of four products in a pixel were identical, 2) the LC types of three products in a pixel were identical, 3) the LC types of two products in a pixel were identical, and 4) the LC types of four products in a pixel were completely different. The formula is as follow:

$$V = \mathrm{int}(L \times 1000 + M \times 100 + N \times 10 + U) \tag{3}$$

where V is the consistency map of the four LC products on TP in 2000, 2010, and 2020; L, M, N, and U represent the LC maps of MCD12Q1, CCI-LC, GlobeLand30, and CNLUCC on the TP in 2000, 2010, and 2020.

3) Google Earth Validation Analysis: The Google Earth platform provides high-resolution satellite images for most locations [46]. Google Earth platform-assisted validation guarantees the accuracy of LC product consistency verification and compensates for the lack of real LC type verification. The land type inconsistency of the four LC products was verified using 24 133 validation points in 2020 on the TP. Since the area of different LC s on TP varies greatly, the number of validation sites selected varies for different LC types. In addition, shrubland on TP can easily be confused with LC types such as grassland and forest [47]. It is challenging to correctly classify shrubland from google platform by visual interpretation. Therefore, the remaining eight types were selected by Google validation. Table III showed the number of validation points for each LC type. First, the ArcGIS (v.10.8) spatial join tool was used to link the google validation dataset to the LC dataset. Second, the attribute table was exported and python 3.0 was used to calculate the area of LC types for which the LC dataset did not match the google validation data. Finally, the percentage of inconsistent area in each LC product were calculated.

4) Change Consistency Analysis: The land transfer matrix is a two-dimensional (2-D) matrix obtained based on the relationship of LC change in the same area at different times. It can not

TABLE III
NUMBER OF GOOGLE VERIFICATION POINTS FOR LAND COVER TYPES

	Forest	Grassland	Cultivated land	Wetland	Water bodies	Artificial surfaces	Snow and ice	Bare land
Verification points number	2018	11932	1113	1009	1338	1240	2275	3208

only indicate the transformation between different LC types, but also quantitatively reflect the transfer rate of different LC types. The formula is

$$S_{ab} = \begin{bmatrix} s_{11} & \cdots & s_{1n} \\ \vdots & \ddots & \vdots \\ s_{n1} & \cdots & s_{nn} \end{bmatrix} \quad (4)$$

where s_{ab} is the specific quantitative of the conversion from LC type a to type b in 2000–2010 or 2010–2020 and n is the number of LC types (n= 9).

Spatial superposition was used to analyze the pixel-by-pixel change consistency of the four LC products. Equation (5) was applied in the raster calculator of ArcGIS (v.10.8) software to calculate the change consistency in the four LC products. The pixel of one and more product changes is defined as change areas after the four LC products are overlaid. The pixel where two or more LC products changed the same was defined as the change consistent area. The superimposed results were filtered with python 3.0 to get the change area and the percentage of change consistent area

$$W = \text{int}(A \times 1000000 + B \times 10000 + C \times 100 + D). \quad (5)$$

In (5), W is the change consistency map for the four products from 2000 to 2010 or from 2010 to 2020;A, B, C, and Drepresent the LC change maps of MCD12Q1, CCI-LC, Globeland30, and CNLUCC products on the TP, respectively.

5) Elevation Heterogeneity Analysis: According to the classification system of geomorphologic atlas of the People's Republic of China (1:1,000,000) [48], the TP was divided into four altitude zones, including low altitude zone ($<$ 1000 m), middle altitude zone (1000–3500 m), high altitude zone (3500–5000 m), and highest altitude zone ($>$ 5000 m). The spatiotemporal consistency of the four LC products within each elevation zone was counted.

IV. RESULTS

A. Comparison of the Patterns of Landcover Pattern

1) Spatial Patterns: The LC types of the TP account for similar proportion size among the four LC products, mainly grassland and bare land, while smaller areas of other LC types and the smallest area of artificial surfaces (see Fig. 2). The average proportion of grasslands in the four LC products was 50.28%, 56.66%, and 55.56% in 2000, 2010, and 2020, respectively. The average proportion of bare land in the four LC products was 34.37%, 27.04%, and 27.86% in 2000, 2010, and 2020, respectively. The area of forest was much smaller than the area of grassland and bare land, while larger than the area of other LC types. Water bodies, permanent snow and ice, cultivated land, shrubland, and artificial surfaces account for less than 5%. The average proportion of water bodies in the four LC products was 1.96%, 1.79%, and 1.92% in 2000, 2010, and 2020, respectively. The average proportion of shrubland in the four LC products was 1.73%, 1.72%, and 1.67% in 2000, 2010, and 2020, respectively. The average proportion of wetland in the four LC products was 0.86%, 0.88%, and 0.89% in 2000, 2010, and 2020, respectively.

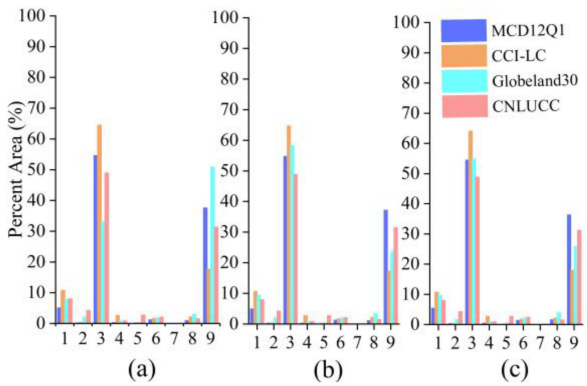

Fig. 2. Percentage of land cover type area for four land cover products in TP (a) 2000 (b) 2010 (c) 2020 (1 forest, 2 shrubland, 3 grassland, 4 cultivated land, 5 wetland, 6 water, 7 artificial surfaces, 8 permanent snow and ice, and 9 bare land).

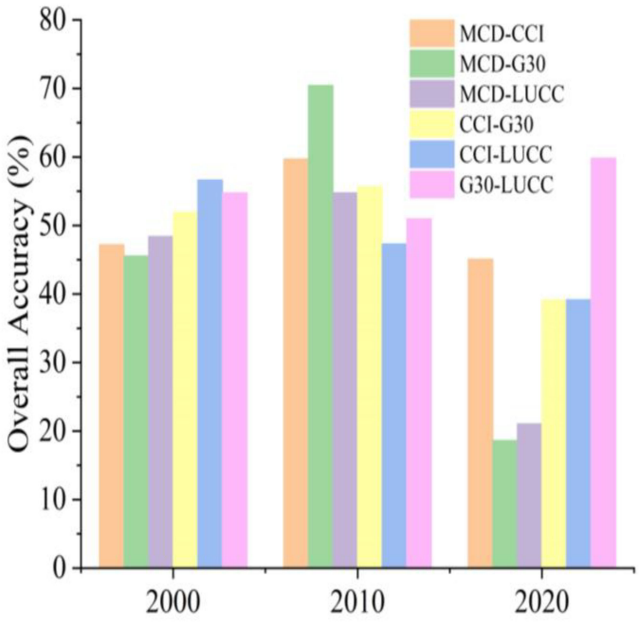

Fig. 3. Overall accuracy of the four land cover products on the TP (MCD: MCD12Q1; CCI: CCI-LC: G30: Globeland30; LUCC: CNLUCC).

2) Classification Accuracy Assessment: The OA of the four LC products in 2000, 2010, and 2020 was less than 75% (see Fig. 3). The average OA value among the four LC products in

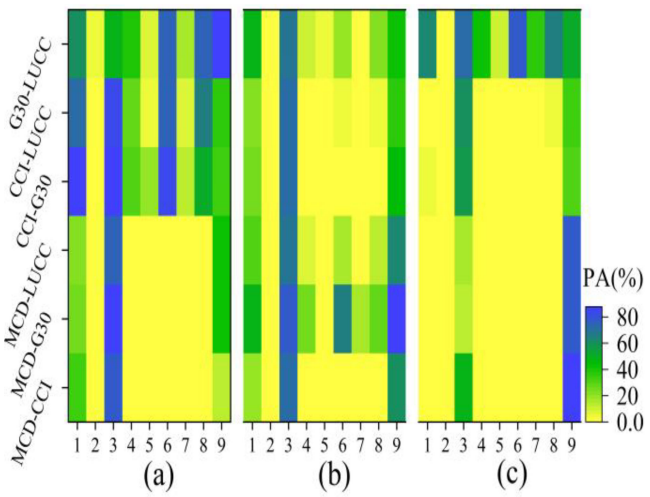

Fig. 4. Producer accuracy of four land cover products on the TP (a) 2000, (b) 2010, (c) 2020 (MCD: MCD12Q1; CCI: CCI-LC: G30: Globeland30; LUCC: CNLUCC) (1 forest, 2 shrubland, 3 grassland, 4 cultivated land, 5 wetland, 6 water, 7 artificial surfaces, 8 permanent snow and ice, and 9 bare land).

2000 was 50.74%. The highest OA between the LC products CNLUCC and CCI-LC (56.64%), followed by Globeland30 and CNLUCC (54.75%). The average OA value in 2010 was 56.47%. The highest OA was found between MCD12Q1 and Globeland30 (70.44%). The second-highest OA was found between CCI-LC and MCD12Q1 (59.71%), while the lowest OA value was found between CNLUCC and CCI-LC (47.31%). The average OA value in 2020 was 37.14%. The highest OA (59.83%) between the LC products CNLUCC and Globeland30. The second-highest OA (46.77%) was between CCI-LC and MCD12Q1, while Globeland30 and MCD12Q1 had the lowest OA (18.63%). Among the four LC products, CCI-LC and Globeland30 had better accuracy, while the accuracy of MCD12Q1 was poor. The OA for the four LC products was generally higher in 2010 than in 2000 and 2020. Therefore, the judgment of OA of the same LC product also required a comprehensive analysis of data over many years.

The mean values of PA varied greatly among LC types in the TP (see Fig. 4). The highest mean PA values were found for grass (70.71%, 69.98%, and 44.32% for 2000, 2010, and 2020, respectively). The mean PA values of bare land were 39.32%, 54.06%, and 51.06% in 2000, 2010, and 2020. The shrubland, wetlands and artificial surfaces had the lowest average PA. Among nine LC types, the mean PA values were higher for grassland (71.78%) and bare land (51.06%), while very low for artificial surfaces (4.95%) and shrubland (0.71%). The mean PA value for the four LC products was generally higher in 2000 (27.85%) than in 2000 (21.81%) and 2020 (17.62%).

3) Spatial and Multiple Location Consistency: The spatial consistency of a single LC type on the TP varies greatly (see Fig. 5). Grassland had the highest spatial consistency. The grassland of consistency with two or more products occupies 74.83%, 80.48%, and 78.97% of the total area of TP in 2000, 2010, and 2020, respectively. The spatial consistency of bare land, water bodies, forests, and permanent snow and ice on the TP ranged from 40% to 70%, while the spatial consistency of cultivated land and the artificial surfaces was lower, both ranging from 10% to 25%. The spatial consistency of wetlands and shrubland was extremely low, both below 10%. The lowest spatial consistency was found in shrubland, with two or more products simultaneously indicated as shrubland in 2000, 2010, and 2020, accounting for 2.15%, 1.69%, and 2.07% of the total TP, respectively.

The spatial consistency of TP shows that the high consistency of four LC products is mainly distributed in the northern and eastern parts of the TP (see Fig. 6). In 2000, 2010, and 2020, 31.9%, 38.67%, and 32.39% of the area of four products in one pixel had the same LC type, respectively. We analyzed the consistency of LC on the TP with a 75% confidence level (75% confidence level means that at least three products have the same LC type in the corresponding pixel), with high confidence levels for 77.11%, 74.67%, and 73.46% of the area in 2000, 2010, and 2020, respectively. However, for the remaining approximately 20% or more of the area, there is still much room to improve the accuracy of the LC remote sensing interpretation products.

4) Google Earth Verification: The four land cover products have different effects on the monitoring and evaluation of LC on the TP (see Fig. 7). Different LC products can be used for monitoring different LC types on the TP. MCD12Q1 was effective in monitoring grassland, cropland and bare land with inconsistencies of 5.85%, 55.56%, and 16.42%, respectively, while it could not be effectively applied to permanent snow and ice, artificial surfaces, and wetland monitoring. CCI-LC has a better monitoring effect on water bodies and artificial surfaces, while a poor monitoring effect on cultivated land. Globeland30 was effective in monitoring forest, wetlands and artificial surfaces. Among the four LC products, low average inconsistency was found for Globeland30 (35.69%) and CCI-LC (40.78%), while both MCD12Q1 and CNLUCC had inconsistencies over 55%.

The inconsistency varies widely among LC types. Grasslands had the lowest average inconsistency (9.98%), while forest (24.53%), bare land (25.15%), and water bodies (30.64%) had less than 35% inconsistency. The inconsistencies of permanent snow and ice (60.49%), artificial surfaces (69.45%), cultivated land (76.38%), and wetland were all above 60%.

B. Comparison of the Patterns of Landcover Change

1) Range of Variation: The LC change maps of the four LC products in 2000–2010 and 2010–2020 were overlaid raster-by-raster to obtain the LC change maps of the four products in the TP (see Fig. 8). We defined the changed area as the total area where at least one LC product has changed. From 2000 to 2010 and from 2010 to 2020, the area of LC change is about 56.16% and 57.01% of the total area on TP, respectively. LC change have become slightly more pronounced than in the previous decade on the TP.

2) Consistency of Change: The area where two and more products changed consistently from 2000 to 2010 accounted for 6.49% change area [see Fig. 8(a)]. The area where two and more products changed consistently from 2010 to 2020 was 119 698 km^2, accounting for 8.15% of the total changed area of the TP [see Fig. 8(b)]. The consistency of LC change on the TP for 2010–2020 was slightly higher than that for 2000–2010.

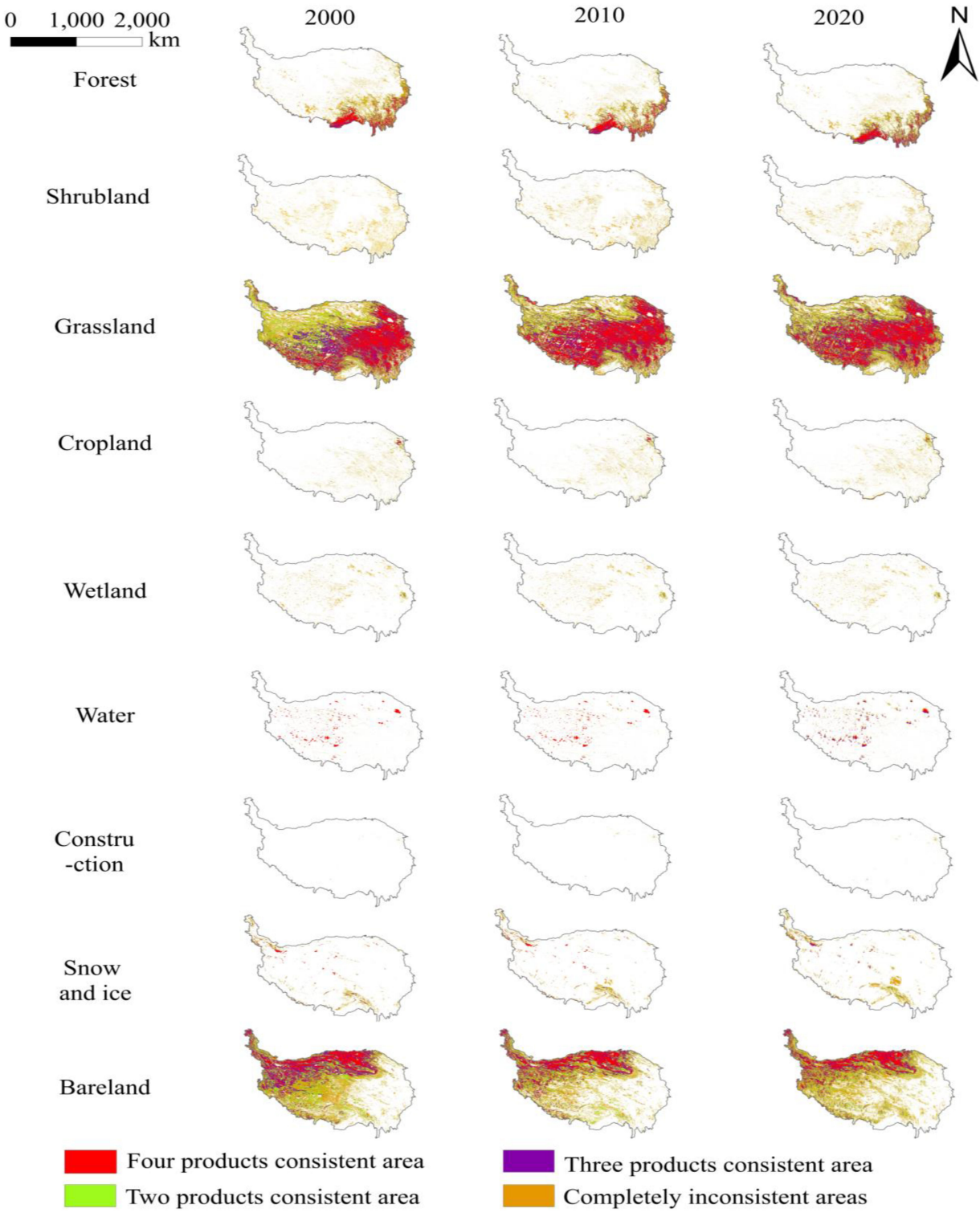

Fig. 5. Spatial consistency of single land cover types on the TP.

Compared with the spatial consistency of the four LC products, the change consistency is extremely low.

C. Elevation Heterogeneity

The average spatial consistency of the four LC products decreased with the increasing elevation [see Fig. 9(a)]. The area of LC change for each elevation zone from 2010 to 2020 is greater than that from 2000 to 2010 [see Fig. 9(b)]. LC change in the higher elevation (high elevation and highest elevation zone) was more pronounced than in the lower elevation (low elevation and middle elevation zone). Similarly, the consistency of LC change was more pronounced at higher elevations than at lower elevations.

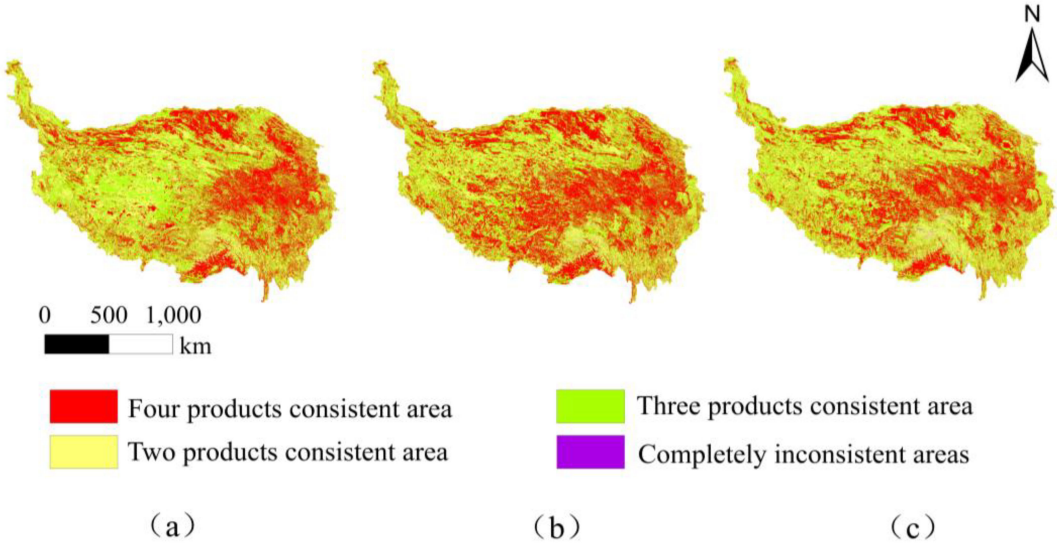

Fig. 6. Spatial consistency of all types of land cover on the TP. (a) 2000. (b) 2010. (c)2020.

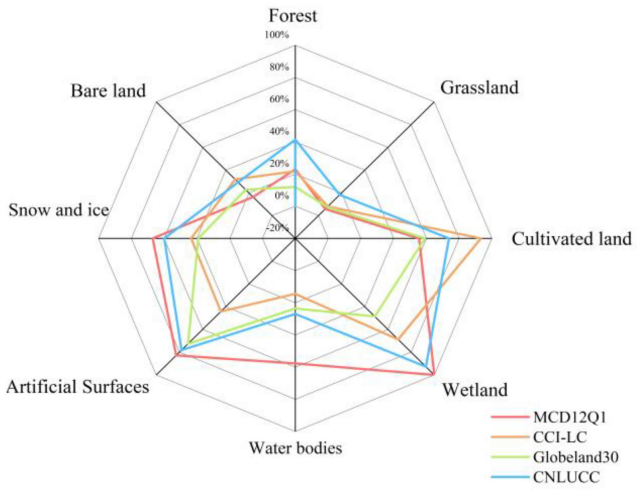

Fig. 7. Inconsistency of Google Earth-assisted verification of land cover types.

V. Discussion

A. Factors Affecting the Spatiotemporal Consistency

The differences between LC products may be real or may be caused by errors in time, classification methods, resolution, and the algorithm when performing the consistency analysis. To exclude the errors caused by the algorithm and time differences, we analyzed the consistency of multisource products through accuracy evaluation, spatial overlay analysis and Google Earth dataset validation. In this article, the LC data of MCD12Q1 products in 2000 and 2020 were replaced by the data in 2001 and 2019. Although temporal differences can have an impact on the consistency analysis of LC, the four LC products can be ignored for consistency analysis. Because the four LC products were superimposed, the spatial consistency of the three and more products was 77.11%, 74.67%, and 73.46% in 2000, 2010, and 2020, respectively. The results showed that temporal differences were not a significant factor in the inconsistency between LC products. Similar results were found for the comparison of consistency between GlobCover and GLCD2005 [26].

The LC classification system is an important factor that affects the consistency of different LC products [46]. The classification systems of MCD12Q1, CCI-LC, and Globeland30 are established for the global LC and CNLUCC is established for the Chinese LC. The four LC products will inevitably produce inconsistencies when applied to the unique flora of the TP. In addition, in order to realize interoperability among them, we have unified the four LC products into nine LC types. Owing to the different classification systems of the four LC products and the different physical definitions of LC in the different classification systems, uniting the four LC products into one classification system will result in error propagation [49]. To reduce the merging error, we use Globeland30 with the fewest LC categories as the benchmark, and merged the LC types of the remaining three LC products into nine categories. Further errors are introduced by grouping confusion categories into similar LC types according to the degree of confusion. For example, in MCD12Q1, woody savannas (tree cover 30%–60%) and savannas (tree cover 10%–30%) are both uniformly classified as grassland. The union of LC types increases the uncertainty in the results of the consistency assessment of the four LC products.

The spatial resolution of the LC product is also important in affecting the consistency [50]. The classification accuracy of LC products is significantly affected by the spatial resolution and the spatial variation increases with the amplification of the spatial resolution [51]. In this article, Google Earth dataset validation found that CCI-LC (300 m) and Globeland30 (30 m) with higher spatial resolution had better consistency compared to MCD12Q1 (500 m) and CNLUCC (1000 m) with lower spatial resolution. Higher resolution products capture more accurately details of the LC, while lower resolution LC products usually lose these details such as rivers and roads. In addition, we adopted an upscaling approach when overlaying the four LC products, using

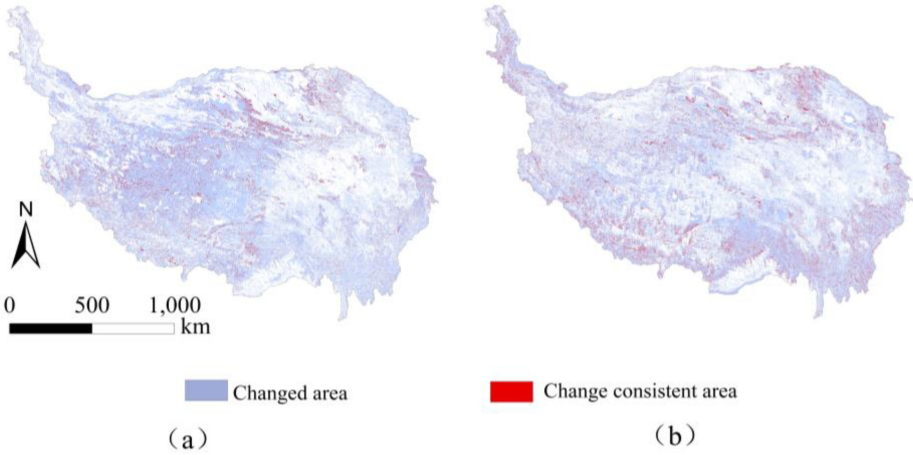

Fig. 8. Consistency of changes in two and more products on the TP. (a) 2000–2010. (b) 2010–2020.

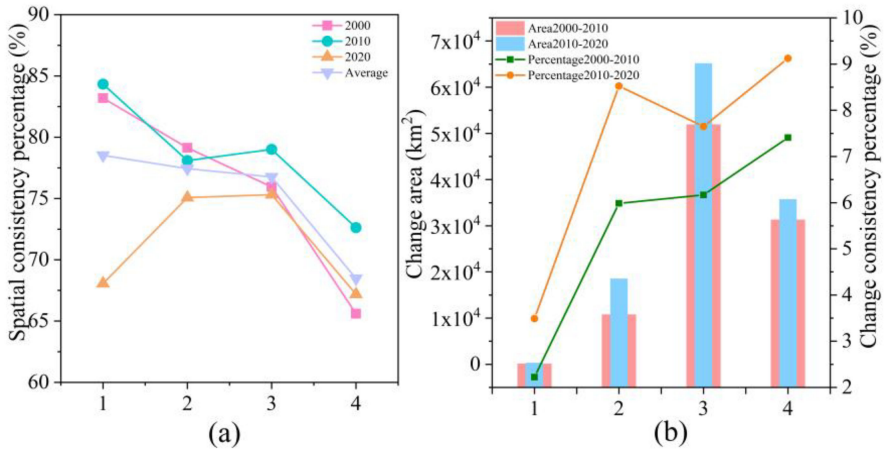

Fig. 9. Spatial and temporal consistency of land cover products in different elevation regions. (a) Spatial consistency. (b) Change area and change consistency (1 low altitude zone, 2 medium altitude zone, 3 high altitude zone, 4 highest altitude zone).

the CNLUCC product as a benchmark, and standardized the spatial resolution of the LC products to 1000 m. Compared to downscaling, upscaling can reduce the problem of mixed pixels to some extent, ensuring that the largest proportion of LC types are represented within each pixel. Moreover, the up-scaling approach can further reduce the amount of data and make the consistency analysis easy to operate. Yet the amplification effect of the main LC types due to the ascending scale can also theoretically bias the results of the LC product consistency assessment.

B. Reasons for Elevation Heterogeneity

The average spatial consistency of the four LC products decreased from low to extreme elevations, indicating that LC inconsistencies were more common and difficult to monitor at higher elevations [52]. Low elevation areas are relatively flat, with low heterogeneity of vegetation, while high elevation topography is complex, with high heterogeneity of features at different resolutions and high inconsistency among LC products [53], [54]. LC changes in the high-altitude (high elevation and highest elevation zone) were more pronounced than in the lower altitude (low elevation and middle elevation zone). The ecological environment in high-altitude areas is fragile, and under the influence of temperature changes, LC changes are more obvious.

C. Recommendations on Improving the Accuracy of LC Products

This article on the spatial consistency of nine LC types on the TP found that the spatial consistency varied greatly among LC types. The spatial consistency of two and more products of grassland, bare land, forest, permanent snow and ice, and water bodies was above 40%, while the spatial consistency of cultivated land, artificial surfaces, wetlands, and shrubs was below 25%. The area of grassland, bare land and forest is large on the TP, easy to identify and relatively high spatial consistency. The interspersed distribution between wetlands and shrubland increases the difficulty of satellite remote sensing monitoring [55]. The low consistency of these LC types has been confirmed not only on the TP but also in other studies. Tsendbazar *et al.*

[3] found the herbaceous wetland class had the lowest class accuracies by validating the global annual LC products. Liang *et al.* [52] found that the LC type with the most difference in classification accuracy between Globeland30 and CCI-LC products in the Arctic was shrubland. Due to the small size of the patches, high internal heterogeneity, and homogeneity, it is difficult to distinguish them from remote sensing images [56]. When map LC types, extra attention should be paid to these special LC types. And the emergence of single-type thematic LC series had provided new ideas for LC studies, such as global artificial impervious area [57], high-resolution global maps of 21st-century forest cover change [58], essential urban land use categories in China (EULUC-China) [59], and 2010 thirty meter resolution forest map for China. The emergence of these thematic maps provides a basis for the study of specific LC types in future studies.

VI. Conclusion

To assess the spatial and temporal consistency of LC products on the TP, we analyzed the consistency of four commonly used four LC products (CCI-LC, GlobeLand30, MCD12Q1, CNLUCC). The spatial consistency of three and four products was less than 80% in 2000, 2010, and 2020, and there were significant differences between different LC types. Spatial consistency was higher than 75% for grassland and bare land, while it was lower than 5% for shrubland. Different LC products have different monitoring effects on LC types. The MCD12Q1 is suitable for monitoring grassland, cultivated land and bare land. The CCI-LC effectively monitor water bodies and artificial surfaces. Globeland30 is better for monitoring forest, wetland, and artificial surfaces. The spatial consistency is high in areas without LC change, while the spatial consistency was extremely low in areas with change. The consistency assessment of LC products is a dynamic process and cannot be judged only by the spatial consistency in a particular year, and it is necessary to strengthen the monitoring of the changing areas on the TP.

Conflicts of interest: The authors declare no conflict of interest.

References

[1] H. Long, Y. Zhang, L. Ma, and S. Tu, "Land use transitions: Progress, challenges and prospects," *Land*, vol. 10, no. 9, Sep. 2021, Art. no. 903, doi: 10.3390/land10090903.

[2] B. L. Turner, E. F. Lambin, and A. Reenberg, "The emergence of land change science for global environmental change and sustainability," *Proc. Nat. Acad. Sci. USA*, vol. 104, no. 52, pp. 20666–20671, Dec. 2007, doi: 10.1073/pnas.0704119104.

[3] N. Tsendbazar *et al.*, "Towards operational validation of annual global land cover maps," *Remote Sens. Environ.*, vol. 266, Dec. 2021, Art. no. 112686, doi: 10.1016/j.rse.2021.112686.

[4] M. A. Wulder, N. C. Coops, D. P. Roy, J. C. White, and T. Hermosilla, "Land cover 2.0," *Int. J. Remote Sens.*, vol. 39, no. 12, pp. 4254–4284, Jun. 2018, doi: 10.1080/01431161.2018.1452075.

[5] A. D. Barnes *et al.*, "Direct and cascading impacts of tropical land-use change on multi-trophic biodiversity," *Nature Ecol. Evol.*, vol. 1, no. 10, pp. 1511–1519, Oct. 2017, doi: 10.1038/s41559-017-0275-7.

[6] K. C. Seto, B. Güneralp, and L. R. Hutyra, "Global forecasts of urban expansion to 2030 and direct impacts on biodiversity and carbon pools," *Proc. Nat. Acad. Sci. USA*, vol. 109, no. 40, pp. 16083–16088, Oct. 2012, doi: 10.1073/pnas.1211658109.

[7] L. E. O. C. Aragão *et al.*, "21st Century drought-Related fires counteract the decline of Amazon deforestation carbon emissions," *Nature Commun.*, vol. 9, no. 1, Dec. 2018, Art. no. 536, doi: 10.1038/s41467-017-02771-y.

[8] K. K. Kusi, A. Khattabi, N. Mhammdi, and S. Lahssini, "Prospective evaluation of the impact of land use change on ecosystem services in the Ourika watershed, Morocco," *Land Use Policy*, vol. 97, Sep. 2020, Art. no. 104796, doi: 10.1016/j.landusepol.2020.104796.

[9] W. Verhagen, A. J. A. van Teeffelen, and P. H. Verburg, "Shifting spatial priorities for ecosystem services in Europe following land use change," *Ecological Indicators*, vol. 89, pp. 397–410, Jun. 2018, doi: 10.1016/j.ecolind.2018.01.019.

[10] Y. Forget, M. Shimoni, M. Gilbert, and C. Linard, "Mapping 20 Years of Urban Expansion in 45 Urban Areas of Sub-Saharan Africa," *Remote Sens.*, vol. 13, no. 3, Feb. 2021, Art. no. 525, doi: 10.3390/rs13030525.

[11] J. van Vliet, "Direct and indirect loss of natural area from urban expansion," *Nature Sustainability*, vol. 2, no. 8, pp. 755–763, Aug. 2019, doi: 10.1038/s41893-019-0340-0.

[12] D. Singh, S. P. McDermid, B. I. Cook, M. J. Puma, L. Nazarenko, and M. Kelley, "Distinct influences of land cover and land management on seasonal Climate," *J. Geophys. Res. Atmos.*, vol. 123, no. 21, pp. 12017–12039, Nov. 2018, doi: 10.1029/2018JD028874.

[13] Z. Zeng *et al.*, "Deforestation-induced warming over tropical mountain regions regulated by elevation," *Nature Geosci.*, vol. 14, no. 1, pp. 23–29, Jan. 2021, doi: 10.1038/s41561-020-00666-0.

[14] B. Tellman *et al.*, "Satellite imaging reveals increased proportion of population exposed to floods," *Nature*, vol. 596, no. 7870, pp. 80–86, Aug. 2021, doi: 10.1038/s41586-021-03695-w.

[15] P. Lacroix, A. Dehecq, and E. Taipe, "Irrigation-Triggered landslides in a Peruvian desert caused by modern intensive farming," *Nature Geosci.*, vol. 13, no. 1, pp. 56–60, Jan. 2020, doi: 10.1038/s41561-019-0500-x.

[16] R. S. Defries and J. R. G. Townshend, "NDVI-derived land cover classifications at a global scale," *Int. J. Remote Sens.*, vol. 15, no. 17, pp. 3567–3586, Nov. 1994, doi: 10.1080/01431169408954345.

[17] M. A. Friedl *et al.*, "MODIS Collection 5 global land cover: Algorithm refinements and characterization of new datasets," *Remote Sens. Environ.*, vol. 114, no. 1, pp. 168–182, Jan. 2010, doi: 10.1016/j.rse.2009.08.016.

[18] P. Defourny *et al.*, "Land Cover CCI: Product user guide version 2," 2018, Accessed: Dec. 4, 2021. [Online]. Available: https://www.esa-landcover-cci.org/?q=webfm_send/84

[19] J. Chen *et al.*, "Global land cover mapping at 30m resolution: A POK-Based operational approach," *ISPRS J. Photogramm. Remote Sens.*, vol. 103, pp. 7–27, May 2015, doi: 10.1016/j.isprsjprs.2014.09.002.

[20] W. Chen, H. Zhao, J. Li, L. Zhu, Z. Wang, and J. Zeng, "Land use transitions and the associated impacts on ecosystem services in the Middle Reaches of the Yangtze River Economic Belt in China based on the geo-informatic Tupu method," *Sci. Total Environ.*, vol. 701, Jan. 2020, Art. no. 134690, doi: 10.1016/j.scitotenv.2019.134690.

[21] H. K. Zhang and D. P. Roy, "Using the 500 m MODIS land cover product to derive a consistent continental scale 30 m Landsat land cover classification," *Remote Sens.*, vol. 197, pp. 15–34, Aug. 2017, doi: 10.1016/j.rse.2017.05.024.

[22] A. Pérez-Hoyos, F. J. García-Haro, and J. San-Miguel-Ayanz, "A methodology to generate a synergetic land-Cover map by fusion of different land-Cover products," *Int. J. Appl. Earth Obs. Geoinf.*, vol. 19, pp. 72–87, Oct. 2012, doi: 10.1016/j.jag.2012.04.011.

[23] K. Liu and E. Xu, "Fusion and correction of multi-source land cover products based on spatial detection and uncertainty reasoning methods in central Asia," *Remote Sens.*, vol. 13, no. 2, Jan. 2021, Art. no. 244, doi: 10.3390/rs13020244.

[24] Y. Zhao *et al.*, "Towards a common validation sample set for global land-cover mapping," *Int. J. Remote Sens.*, vol. 35, no. 13, pp. 4795–4814, Jul. 2014, doi: 10.1080/01431161.2014.930202.

[25] T. Hua, W. Zhao, Y. Liu, S. Wang, and S. Yang, "Spatial consistency assessments for global land-cover datasets: A comparison among GLC2000, CCI LC, MCD12, GLOBCOVER and GLCNMO," *Remote Sens.*, vol. 10, no. 11, Nov. 2018, Art. no. 1846, doi: 10.3390/rs10111846.

[26] Y. Bai, M. Feng, H. Jiang, J. Wang, Y. Zhu, and Y. Liu, "Assessing consistency of five global land cover data sets in China," *Remote Sens.*, vol. 6, no. 9, pp. 8739–8759, Sep. 2014, doi: 10.3390/rs6098739.

[27] J. Kang, Z. Wang, L. Sui, X. Yang, Y. Ma, and J. Wang, "Consistency analysis of remote sensing land cover products in the tropical rainforest climate region: A case study of Indonesia," *Remote Sens.*, vol. 12, no. 9, Apr. 2020, Art. no. 1410, doi: 10.3390/rs12091410.

[28] A. T. Kaptué Tchuenté, J.-L. Roujean, and S. M. De Jong, "Comparison and relative quality assessment of the GLC2000, GLOBCOVER, MODIS and ECOCLIMAP land cover data sets at the African continental scale," *Int. J. Appl. Earth Observ. Geoinformation*, vol. 13, no. 2, pp. 207–219, Apr. 2011, doi: 10.1016/j.jag.2010.11.005.

[29] M. Cheng, J. Jin, J. Zhang, H. Jiang, and R. Wang, "Effect of climate change on vegetation phenology of different land-cover types on the Tibetan Plateau," *Int. J. Remote Sens.*, vol. 39, no. 2, pp. 470–487, Jan. 2018, doi: 10.1080/01431161.2017.1387308.

[30] W. Jiang, Y. Lü, Y. Liu, and W. Gao, "Ecosystem service value of the Qinghai-Tibet Plateau significantly increased during 25 years," *Ecosystem Serv.*, vol. 44, Aug. 2020, Art. no. 101146, doi: 10.1016/j.ecoser.2020.101146.

[31] C. Wang, Q. Gao, and M. Yu, "Quantifying trends of Land change in Qinghai-Tibet Plateau during 2001–2015," *Remote Sens.*, vol. 11, no. 20, Oct. 2019, Art. no. 2435, doi: 10.3390/rs11202435.

[32] Z. Wang *et al.*, "Quantitative assess the driving forces on the grassland degradation in the Qinghai-Tibet Plateau, in China," *Ecological Inform.*, vol. 33, pp. 32–44, May 2016, doi: 10.1016/j.ecoinf.2016.03.006.

[33] M. Yang, X. Wang, G. Pang, G. Wan, and Z. Liu, "The Tibetan Plateau cryosphere: Observations and model simulations for current status and recent changes," *Earth Sci. Rev.*, vol. 190, pp. 353–369, Mar. 2019, doi: 10.1016/j.earscirev.2018.12.018.

[34] Y. Wang, B. Fu, Y. Liu, Y. Li, X. Feng, and S. Wang, "Response of vegetation to drought in the Tibetan Plateau: Elevation differentiation and the dominant factors," *Agric. Meteorol.*, vol. 306, Aug. 2021, Art. no. 108468, doi: 10.1016/j.agrformet.2021.108468.

[35] H. Liu *et al.*, "Shifting plant species composition in response to climate change stabilizes grassland primary production," *Proc. Nat. Acad. Sci. USA*, vol. 115, no. 16, pp. 4051–4056, Apr. 2018, doi: 10.1073/pnas.1700299114.

[36] Y. Ran, X. Li, and G. Cheng, "Climate warming over the past half century has led to thermal degradation of permafrost on the Qinghai–Tibet Plateau," *Cryosphere*, vol. 12, no. 2, pp. 595–608, Feb. 2018, doi: 10.5194/tc-12-595-2018.

[37] S. Piao *et al.*, "The impacts of climate change on water resources and agriculture in China," *Nature*, vol. 467, no. 7311, pp. 43–51 Sep. 2010, doi: 10.1038/nature09364.

[38] P. Wang *et al.*, "Increased annual methane uptake driven by warmer winters in an alpine meadow," *Glob. Change Biol.*, vol. 28, no. 10, pp. 3246–3259, 2022, doi: 10.1111/gcb.16120.

[39] Y. Gao, L. Liu, X. Zhang, X. Chen, J. Mi, and S. Xie, "Consistency analysis and accuracy assessment of three global 30-m Land-Cover products over the european union using the LUCAS dataset," *Remote Sens.*, vol. 12, no. 21, Oct. 2020, Art. no. 3479, doi: 10.3390/rs12213479.

[40] C. Chirachawala, S. Shrestha, M. S. Babel, S. G. P. Virdis, and S. Wichakul, "Evaluation of global land use/land cover products for hydrologic simulation in the Upper Yom River Basin, Thailand," *Sci. Total Environ.*, vol. 708, Mar. 2020, Art. no. 135148, doi: 10.1016/j.scitotenv.2019.135148.

[41] J. Kang, L. Sui, X. Yang, Z. Wang, C. Huang, and J. Wang, "Spatial pattern consistency among different remote-sensing land cover datasets: A case study in Northern Laos," *Int. J. Geo-Inf.*, vol. 8, no. 5, May 2019, Art. no. 201, doi: 10.3390/ijgi8050201.

[42] G. M. Foody, "Assessing the accuracy of land cover change with imperfect ground reference data," *Remote Sens. Environ.*, vol. 114, no. 10, pp. 2271–2285, Oct. 2010, doi: 10.1016/j.rse.2010.05.003.

[43] S. V. Stehman, "Sampling designs for accuracy assessment of land cover," *Int. J. Remote Sens.*, vol. 30, no. 20, pp. 5243–5272, Sep. 2009, doi: 10.1080/01431160903131000.

[44] J. Chen *et al.*, "Collaborative validation of GlobeLand30: Methodology and practices," *Geo-Spatial Inf. Sci.*, vol. 24, no. 1, pp. 134–144, Jan. 2021, doi: 10.1080/10095020.2021.1894906.

[45] X. Zhang, L. Liu, X. Chen, Y. Gao, S. Xie, and J. Mi, "GLC_FCS30: Global land-cover product with fine classification system at 30 m using time-series Landsat imagery," *Earth Syst. Sci. Data*, vol. 13, no. 6, pp. 2753–2776, Jun. 2021, doi: 10.5194/essd-13-2753-2021.

[46] H. Gilani *et al.*, "Decadal land cover change dynamics in Bhutan," *J. Environ. Manage*, vol. 148, pp. 91–100, Jan. 2015, doi: 10.1016/j.jenvman.2014.02.014.

[47] B. Ayhan and C. Kwan, "Tree, Shrub, and Grass classification using only RGB images," *Remote Sens.*, vol. 12, no. 8, Apr. 2020, Art. no. 1333, doi: 10.3390/rs12081333.

[48] W. Cheng, C. Zhou, H. Chai, S. Zhao, H. Liu, and Z. Zhou, "Research and compilation of the geomorphologic atlas of the People's Republic of China (1:1,000,000)," *J. Geographical Sci.*, vol. 21, no. 1, pp. 89–100, Feb. 2011, doi: 10.1007/s11442-011-0831-z.

[49] A. Huang, R. Shen, Y. Li, H. Han, W. Di, and D. F. T. Hagan, "A methodology to generate integrated land cover data for land surface model by improving Dempster-Shafer theory," *Remote Sens.*, vol. 14, no. 4, Feb. 2022, Art. no. 972, doi: 10.3390/rs14040972.

[50] H. Wang, L. Cai, X. Wen, D. Fan, and Y. Wang, "Land cover change and multiple remotely sensed datasets consistency in China," *Ecosyst. Health Sustainability*, vol. 8, no. 1, Dec. 2022, Art. no. 2040385, doi: 10.1080/20964129.2022.2040385.

[51] K. Xu, Q. Tian, Y. Yang, J. Yue, and S. Tang, "How up-scaling of remote-sensing images affects land-cover classification by comparison with multiscale satellite images," *Int. J. Remote Sens.*, vol. 40, no. 7, pp. 2784–2810, Apr. 2019, doi: 10.1080/01431161.2018.1533656.

[52] L. Liang, Q. Liu, G. Liu, H. Li, and C. Huang, "Accuracy Evaluation and Consistency Analysis of Four Global Land Cover Products in the Arctic Region," *Remote Sens*., vol. 11, no. 12, Jun. 2019, Art. no. 1396, doi: 10.3390/rs11121396.

[53] L. Wang and J. Jin, "Uncertainty Analysis of Multisource Land Cover Products in China," *Sustainability*, vol. 13, no. 16, Jan. 2021, Art. no. 8857, doi: 10.3390/su13168857.

[54] F. Song *et al.*, "Multi-Scale feature based land cover change detection in mountainous terrain using multi-temporal and multi-Sensor remote sensing images," *IEEE Access*, vol. 6, pp. 77494–77508, 2018, doi: 10.1109/ACCESS.2018.2883254.

[55] Y. Xu *et al.*, "Comparisons of three recent moderate resolution African land cover datasets: CGLS-LC100, ESA-S2-LC20, and FROM-GLC-Africa30," *Int. J. Remote Sens.*, vol. 40, no. 16, pp. 6185–6202, Aug. 2019, doi: 10.1080/01431161.2019.1587207.

[56] I. Soubry and X. Guo, "Identification of the optimal season and spectral regions for shrub cover estimation in Grasslands," *Sensors*, vol. 21, no. 9, Jan. 2021, Art. no. 3098, doi: 10.3390/s21093098.

[57] P. Gong *et al.*, "Annual maps of global artificial impervious area (GAIA) between 1985 and 2018," *Remote Sens. Environ.*, vol. 236, Jan. 2020, Art. no. 111510, doi: 10.1016/j.rse.2019.111510.

[58] M. C. Hansen *et al.*, "High-Resolution Global Maps of 21st-Century forest cover change," *Science*, vol. 342, no. 6160, pp. 850–853, Nov. 2013, doi: 10.1126/science.1244693.

[59] P. Gong *et al.*, "Mapping essential urban land use categories in China (EULUC-China): Preliminary results for 2018," *Sci. Bull.*, vol. 65, no. 3, pp. 182–187, Feb. 2020, doi: 10.1016/j.scib.2019.12.007.